JOURNAL OF MATERIALS SCIENCE 18 (1983) 1629–1637

An intergrown perovskite–wollastonite phase in some ferrous blast-furnace slags

E. WEARING*
Department of Geology and Mineralogy, Oxford University, Parks Road, Oxford, UK

During crystallization of silicate liquids, TiO_2 tends to form its own mineral. Ferrous blast-furnace slags generally have perovskite as the titanium-rich phase. However, a rounded and fibrous phase, crystallizing instead of perovskite, has been observed in some slag samples: it has an apparently late position in the order of crystallization. Detailed electron microprobe analysis and X-ray diffraction have indicated that this unusual phase is composed of intergrown perovskite and wollastonite. However, wollastonite should not be an equilibrium phase in these slags. Therefore, a series of simple high-temperature furnace experiments were conducted to examine possible origins of this intergrowth. Solid solution, liquid immiscibility, and eutectic growth have all been discounted as possible explanations of the intergrowth. However, blast-furnace slags are non-equilibrium products, and their residual liquids crystallize independently. This intergrown perovskite–wollastonite phase has been accounted for as a product of fractional crystallization within the system $CaO–MgO–Al_2O_3–TiO_2–SiO_2$.

1. Introduction

If metallurgical slags are cast into ladles and allowed to cool slowly prior to tipping (1 to 5 days approximately), the resulting solid slags are crystalline and generally suitable for a mineralogical investigation. Some slowly-cooled samples of ferrous blast-furnace slags, from the Port Talbot works of the British Steel Corporation, have been mineralogically examined: their bulk compositions belong essentially to the system CaO(C)–MgO(M)–Al_2O_3(A)–SiO_2(S). They have crystallized minerals such as melilite ($C_2AS–C_2MS_2$ solid solution), monticellite (CMS), merwinite (C_3MS_2), forsterite (M_2S), and spinel (MA); accessory perovskite, nepheline, and phlogopite can also crystallize.

During the crystallization of silicate liquids, there is usually an absence of suitable minerals into which TiO_2 can substitute. Hence, TiO_2(T) tends to form its own mineral, which can be either sphene (CTS) or perovskite (CT) or a Fe–Ti oxide. In these blast-furnace slags, perovskite is generally the titanium-rich phase. However, in two samples (numbers 1370 and 1760) a rounded, fibrous mineral has crystallized instead of the perovskite. A search of the mineralogical literature indicates that there has been no previous description of an equivalent mineral phase. Therefore, this rounded mineral requires an examination as to its possible origin.

2. Techniques

The textural relationships between the minerals have been established by detailed microscopic examination. The mineral chemistry was established by electron microprobe analysis, using a CSI Microscan 9 instrument: on-line computer corrections for mass absorption, atomic number, and secondary fluorescence effects were applied to all raw data. Bulk compositions were determined by X-ray fluorescence, using a Philips 1410 spectrometer with an on-line computer to record the results and correct for mass absorption and secondary fluorescence effects.

---

*Present address: 210 Wingrove Road, Newcastle upon Tyne, NE4 9DD, UK.

0022–2461/83 $03.00 + .12

3. Mineralogy of the rounded phase

In thin-section, this rounded titanium-rich mineral (up to 0.05 mm x 0.05 mm in size) has a brown body colour, which is similar to that of the perovskite in the other samples. The fibrous structure is formed by numerous parallel fibres which appear to have high relief and show a wavy extinction position. The birefringence of these fibres appears to be of high order, but is probably masked by the brown body colour.

Electron microprobe analyses of this phase (Table I) show the presence of substantial amounts of CaO and TiO_2 (indicating perovskite) and SiO_2 (due to a silicate). Therefore, the chemistry indicates the presence of a silicate (the fibres) with perovskite. The term "pseudo-perovskite" will be used to refer to this phase.

In Sample 1370 melilite, merwinite, monticellite and spinel have crystallized with the pseudo-perovskite, whilst in Sample 1760 the other crystalline products are melilite and merwinite. The overall textural relationship between pseudo-perovskite and the melilite, merwinite and monticellite is inconclusive. However, this rounded

TABLE I Electron microprobe analyses of pseudo-perovskite in Samples 1370 and 1760, and an analysis (1369A) of perovskite

	Analysis					
	1370A	1370B	1370C	1760A	1760B	1369A
Composition in oxides						
SiO_2	10.73	9.14	8.10	8.83	3.58	0.00
Al_2O_3	1.32	1.58	1.41	1.44	1.16	1.15
TiO_2	37.36	39.32	42.07	40.77	48.50	53.69
MgO	3.35	2.98	2.31	2.92	1.35	0.14
FeO	0.00	0.06	0.06	0.00	0.01	0.00
MnO	0.00	0.00	0.00	0.07	0.05	0.00
CaO	42.12	41.79	41.87	42.84	41.25	37.07
Na_2O	0.52	0.19	0.38	0.15	0.15	0.38
K_2O	0.07	0.07	0.06	0.15	0.18	0.07
Cr_2O_3	0.07	0.00	0.05	0.00	0.00	0.11
V_2O_3	0.11	0.05	0.09	0.00	0.00	0.38
La_2O_3	0.17	0.27	0.05	0.05	0.01	1.34
Ce_2O_3	0.39	0.84	0.39	0.35	0.24	2.36
Nd_2O_3	0.00	0.15	0.00	0.07	0.07	0.73
Sm_2O_3	0.00	0.00	0.00	0.02	0.00	0.15
Gd_2O_3	0.00	0.00	0.00	0.08	0.07	0.11
Y_2O_3	0.00	0.00	0.00	0.24	0.32	0.40
Total	96.21	96.44	96.84	97.98	96.94	98.08
Structural formula based on 3 oxygens						
Si	0.245	0.210	0.185	0.200	0.083	0.000
Al	0.036	0.043	0.038	0.038	0.032	0.032
Ti	0.642	0.680	0.724	0.694	0.847	0.956
Mg	0.114	0.102	0.079	0.098	0.047	0.005
Fe^{2+}	0.000	0.001	0.001	0.000	0.000	0.000
Mn	0.000	0.000	0.000	0.001	0.001	0.000
Ca	1.032	1.029	1.026	1.039	1.027	0.940
Na	0.023	0.008	0.017	0.007	0.007	0.017
K	0.002	0.002	0.002	0.004	0.005	0.002
Cr	0.001	0.000	0.001	0.000	0.000	0.002
V^{3+}	0.002	0.001	0.001	0.000	0.000	0.006
La^{3+}	0.001	0.002	0.000	0.000	0.000	0.012
Ce^{3+}	0.003	0.007	0.003	0.003	0.002	0.020
Nd^{3+}	0.000	0.001	0.000	0.001	0.001	0.006
Sm^{3+}	0.000	0.000	0.000	0.000	0.000	0.001
Gd^{3+}	0.000	0.000	0.000	0.001	0.001	0.001
Y^{3+}	0.000	0.000	0.000	0.003	0.004	0.005
Total	2.101	2.086	2.077	2.089	2.057	2.006

phase tends to crystallize at the grain boundaries and triple points of the other phases, which suggests a late position in the order of crystallization (Fig. 1).

4. Chemical characteristics

Comparing analyses 1370A–C and 1760A–B (Table I) with that for a typical perovskite from blast-furnace slags (analysis 1369A), the pseudo-perovskite has a slightly higher Al_2O_3 content than ordinary perovskite. This can probably be explained by some Al^{3+} substituting into four-fold sites of the silicate. The depleted TiO_2 content of pseudo-perovskite can be attributed to the dilution of the perovskite in the analysis by the silicate phase. The pseudo-perovskite has a higher CaO content which suggests that CaO is a major component in the silicate phase, and that there is no substitution of rare-earth elements for Ca^{2+} in the silicate since the rare-earth elements are depleted compared to analysis 1369A. Although MgO is taken up into the perovskite structure in small amounts, its presence seems likely to be related to the silicate.

Therefore, the important oxides in determining the proportions of silicate in perovskite are CaO, MgO, Al_2O_3, TiO_2 and SiO_2. Assuming that all the SiO_2 is in the silicate and all the TiO_2 in the perovskite, analysis 1369A can be used to calculate the perovskite contribution in the pseudo-perovskite analyses. The remainder can be taken as representing the silicate, and so by normalizing to 100%, compositions can be calculated (Table II). Errors will be expected because the analysis totals are low, and the oxide partition coefficients between the two phases are unknown. Analysis 1370A has the highest SiO_2 content, which corresponds to a composition of silicate$_{27.3}$ perovskite$_{72.7}$. From Table II the composition of the silicate is between $CaSiO_3$ and Ca_2SiO_4, and allowing for errors merwinite seems possible.

5. X-ray diffraction data

A diffraction pattern for pseudo-perovskite was

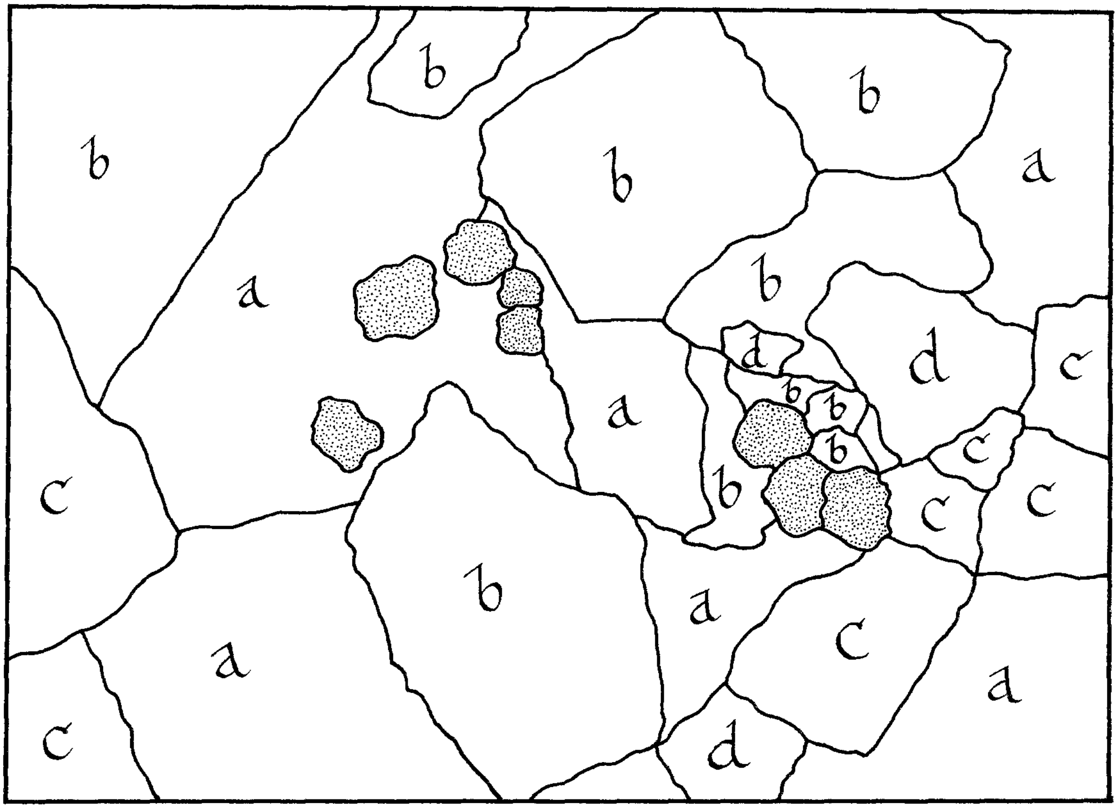

Figure 1 Sketch photomicrograph from sample 1370 illustrating the tendency of the rounded pseudo-perovskite (stippled) to crystallize at the grain boundaries and triple points of melilite (a), monticellite (b), merwinite (c), and spinel (d). The field of view is 1.0 mm across.

TABLE II Calculated composition of the silicate component in pseudo-perovskite

	Analysis					
	1370A		1370C		1760B	
Composition in oxides						
SiO_2	39.33		38.72		44.03	
Al_2O_3	1.91		6.74		1.72	
MgO	11.91		10.28		15.01	
CaO	46.85		44.26		39.24	
Total	100.00		100.00		100.00	
Number of cations for 3 oxygens						
Si	0.79	0.84	0.76	0.92	0.85	0.89
Al	0.05		0.16		0.04	
Mg	0.35	1.35	0.30	1.24	0.43	1.24
Ca	1.00		0.94		0.81	
Number of cations for 4 oxygens						
Si	1.05	1.11	1.02	1.23	1.13	1.18
Al	0.06		0.21		0.05	
Mg	0.47	1.80	0.40	1.65	0.57	1.65
Ca	1.33		1.25		1.08	

obtained from the Gandolfi single-crystal camera, which has the lines of perovskite (obtained from a brown perovskite crystal in Sample 1369) plus other lines (Table III). These extra lines are assumed to be from the silicate phase, but they do not correspond to the diffraction patterns for the other known silicates in ferrous blast-furnace slags. This removes the possibility of merwinite. However, the extra lines closely match the strong lines for α-wollastonite, but not those for dicalcium silicate. To check the reliability of this identification a mixture representing 20 mol% wollastonite–80 mol% perovskite was prepared from powders, and the resulting diffraction pattern was obtained from a diffractometer. This compares favourably to that for the pseudo-perovskite. Wollastonite is known to be fibrous and has second-order interference colours, which correspond to the fibres in pseudo-perovskite. If the silicate is wollastonite, the MgO can be explained by magnesium replacing calcium.

6. Origin of the wollastonite

Perovskite is known to have a simple eutectic at 1425° C with wollastonite. However, from the position of these slags in the system $CaO-MgO-Al_2O_3-SiO_2$, and using the quaternary liquidus diagrams of Osborn *et al.* [1], this eutectic cannot be present since wollastonite is unlikely to be an equilibrium phase.

There are three possible origins for the crystallization of the wollastonite, without it being an equilibrium phase.

1. There may be a perovskite solid solution with wollastonite, which is stable in the presence of melilite, monticellite and merwinite, even though wollastonite alone is not.
2. Liquid immiscibility is widespread in silica–titania systems, which could result in the separation of a TiO_2-rich immiscible liquid. This could then crystallize out as perovskite + wollastonite.
3. The pseudo-perovskite-bearing samples have a low TiO_2 bulk content relative to those crystallizing ordinary perovskite. Therefore, a greater proportion of crystallization of the slag is required before the TiO_2 content of the residual liquid is high enough for the crystallization of perovskite. The residual liquid composition may be close to the perovskite–wollastonite system, and so the pseudo-perovskite could represent eutectic growth.

These three possibilities have been investigated by simple high-temperature furnace experiments.

7. High-temperature experiments

7.1. Solid solution

The first set of experimental runs was to examine the possibility of solid solution between wollastonite and perovskite at high temperature. At lower temperatures the two would exsolve to give the fibrous structure. However, no evidence of silicate solubility in perovskite at atmospheric pressure has been reported, and from crystal-chemical considerations substitution of Si^{4+} for Ti^{4+} would not be expected at this pressure. Ringwood and Major [2] reported solubility of up to 83 mol% wollastonite in perovskite at a pressure of 2.5×10^{10} Nm^{-2}. DeVries *et al.* [3] investigated the system $CaTiO_3-CaSiO_3$ at atmospheric pressure, which forms a eutectic at 1425° C, but found no evidence for solid solution at the $CaTiO_3$ end.

Powders of perovskite (Per) and wollastonite (Wo) were used as the starting materials for the experimental runs (Table IV). However, the run temperatures would have been above the inversion temperature to pseudo-wollastonite, and so the wollastonite was inverted before addition to the pervoskite. A composition of $Per_{90}Wo_{10}$ (the diffraction peaks of the two phases can be distinguished in the starting material) heated to high temperatures (Runs 1 to 3) has

TABLE III Comparison of X-ray diffraction patterns for perovskite, pseudo-perovskite and the mixture wollastonite$_{20}$–perovskite$_{80}$ (Wo = wollastonite and Per = perovskite)

Perovskite (Sample 1369)		Pseudo-perovskite (Sample 1370)		Diffractometer trace (Sample Wo_{20}–Per_{80})		
Estimated I/I_0	d(nm)	Estimated I/I_0	d(nm)	Estimated I/I_0	d(nm)	Line
				1	0.768	Per
1	0.3821	2	0.3820	3	0.3821	Per + Wo
		2	0.3512	2	0.3510	Wo
1 −	0.3415			1	0.3423	Per
		2	0.3312	2	0.3312	Wo
		3	0.3090	1 +	0.3080	Wo
1	0.3028					
3 +	0.2876	2	0.2837	1 −	0.2843	Per
10	0.2699	10	0.2690	10	0.2701	Per
1 − −	0.2597	1	0.2585			Per
		2	0.2553	1	0.2553	Wo
				1 − −	0.2470	Wo
				1 −	0.2428	Per
2	0.2417	3	0.2399	2	0.2413	Per
				1	0.2349	Wo
2 +	0.2304	2	0.2296			Per
3	0.2212	5	0.2205	1	0.2210	Per
				1 − −	0.2170	Wo
1 +	0.2113	1 −	0.2125	1	0.2121	Per
1 +	0.2041			1 −	0.2050	Per
		1	0.2014	1 −	0.2017	Wo
8	0.1910	10	0.1908	6	0.1911	Per
		1 −	0.1852	1 −	0.1856	Wo
1 − −	0.1818	1 −	0.1815			Per
		1 −	0.1759	1	0.1758	Wo
1	0.1756	1 −	0.1751	1	0.1750	Per
1 −	0.1707	1 +	0.1720	1	0.1717	Per + Wo
1 −	0.1670			1	0.1676	Per
		2 +	0.1599	2 −	0.1600	Wo
10	0.1561	10	0.1559	2	0.1560	Per
				1 −	0.1533	Wo
		2 −	0.1509	1 −	0.1512	Wo
				1 −	0.147 41	Wo
		1	0.142 84	1 −	0.142 91	Wo
		1	0.138 97	1 −	0.138 81	Wo
5	0.135 09	8	0.134 81	2	0.135 07	Per
		1	0.126 61	1	0.126 54	Wo
5	0.120 81	5	0.120 84	2	0.120 81	Per
		1 − −	0.116 00	1 − −	0.116 22	Wo
1 − −	0.110 78	1 +	0.110 78	1 −	0.110 71	Per

only perovskite peaks on quenching. This suggests that the $CaSiO_3$ has been taken up into solid solution by the $CaTiO_3$.

A composition of $Per_{80}Wo_{20}$ (Run 4) produced peaks of perovskite and pseudo-wollastonite. This product was re-annealed at a lower temperature (Run 5) to see if there was exsolution. The ratio between the main wollastonite and perovskite peaks increased from 0.11 (Run 4) to 0.15 (Run 5), which suggests an increase of wollastonite relative to perovskite during annealing. Although this could be a feature of exsolution, the wollastonite crystals may also have increased in size during annealing, which would increase the intensity of the reflections relative to perovskite.

Crystal growth does not occur during this type of powder experiment, and so the individual phases cannot be analysed. Because the evidence is not conclusive, experiments are required which enable crystal growth to occur. To do this, a flux has to be added to the powders so that the liquidus

TABLE IV Listing of experimental runs, used to examine a possible perovskite–wollastonite solid solution

Run*	Time (h)	Wo (mol %)	Temperature (° C)	Products
1	96	10	1420	Perovskite
2	96	10	1350	Perovskite
3	22	10	1350	Perovskite
4	22	20	1350	Pseudo-wollastonite, perovskite
5	22	20	1200	Pseudo-wollastonite, perovskite
6	72	20†	1150	Perovskite
7	72	20‡	1150	Perovskite

*Runs 1 to 5 were carried out by suspending a platinum capsule (containing the sample) inside a high-temperature experimental furnace. Runs 6 to 7 were carried out by placing a platinum crucible (containing the sample) inside a box-furnace.

†With 4 mol % LiF flux in addition.

‡With 4 % of sample 1370 in addition (to act as a flux).

temperature is reached. Two types of flux were used; LiF (Run 6) and some slag (Sample 1370, Run 7). The products from both runs were perovskite + residual liquid. Electron microprobe work showed no trace of silicate within the perovskite. This observation agrees with the work of DeVries *et al.* [3] and with the crystal-chemical considerations. Therefore, this pseudo-perovskite is not connected with solid solution.

7.2. Possible liquid immiscibility (Table V)

To investigate liquid immiscibility within blast-furnace slags, some powder from Sample 1370 was used for the experiments. To increase the possibility of liquid immiscibility, 5 mol % $CaTiO_3$ was added to the slag (Runs A, B and B2). The sample was heated in a platinum crucible at 1220° C to attain the liquidus temperature, and then slowly cooled over 48 h to simulate crystallization within a ladle.

The products from these experiments were melilite, merwinite, monticellite, spinel and perovskite. However, their proportions are different from Sample 1370, which is probably a result of loss of S, Na_2O and K_2O during heating, and this would slightly change the composition of the slag. There is no evidence of liquid immiscibility within sample 1370, dependent on the TiO_2 content of the liquid.

A region of liquid immiscibility in these slags would presumably cover a range of SiO_2-rich and TiO_2-rich compositions. Since the slags are lime-rich substances, any liquid immiscibility would probably give rise to crystalline SiO_2 and there is no petrographic evidence for this. Liquid immiscibility is therefore an unlikely explanation of pseudo-perovskite, which is supported by the absence of suspended immiscible droplets in all the experimental runs.

7.3. Residual liquid control (Tables V and VI)

Some powder from Sample 1370 was experimentally crystallized (Runs C, D and E) in a similar way to that described for the liquid immiscibility experiments. The pseudo-perovskite was reproduced in Runs D and E as small, rounded, brown crystals (up to 0.10 mm across) with birefringent fibres. The pseudo-perovskite forms less than 0.1 vol % of the crystalline product, and occurs between crystals as in Samples 1370 and 1760. It is positionally distinct from the glass representing definite residual liquid.

Typical compositions for the glass (representing residual liquid) and the pseudo-perovskite of experimental Run D are given in Table VI. This residual liquid composition is not close to the perovskite–wollastonite system,

TABLE V Listing of experimental runs, used to examine (a) possible liquid immiscibility, and (b) possible residual liquid control for the origin of pseudo-perovskite

Run	Flux with sample (mol %)	Products
(a) A	+ 4 mol % LiF flux	Melilite, merwinite, monticellite, spinel, perovskite, glass
B	no flux	
B2	no flux	
(b) C	+ 4 mol % LiF flux	Melilite, merwinite, monticellite, spinel, glass
D	no flux	Melilite, merwinite, monticellite, spinel, glass, pseudo-perovskite
E	no flux	

TABLE VIA Chemical compositions of some of the phases in experimental Run D

	Composition in oxides			
	Residual liquid (glass)	Pseudo-perovskite	Number of cations for 3 oxygens	
SiO_2	28.84	4.34	Si	0.100
Al_2O_3	16.22	2.87	Al	0.078
TiO_2	4.42	45.37	Ti	0.786
MgO	6.82	1.52	Mg	0.052
MnO	0.39	0.81	Mn	0.016
CaO	34.42	42.19	Ca	1.042
Na_2O	0.66	0.02	Na	0.001
K_2O	0.53	0.01	K	0.000
Total	92.30	97.13	Total	2.075

and there is no chemical evidence for another residual liquid. It is unlikely that fractional crystallization could produce two different residual liquids. Therefore, the pseudo-perovskite cannot represent eutectic growth.

8. Explanation of pseudo-perovskite

8.1. The system $CaO-MgO-Al_2O_3-TiO_2-SiO_2$

The TiO_2 bulk content of ferrous blast-furnace slags varies considerably between samples (0.30 to 2.16 wt% TiO_2), and that of Samples 1370 and 1760 are amongst the lowest (see Table VII). During crystallization, the residual liquids of blast-furnace slags are progressively enriched in TiO_2. From Table VII, Samples 1370 and 1760 require a greater enrichment of TiO_2 before the residual liquid can crystallize perovskite, and so explains the apparent late crystallization of pseudo-perovskite. However, other samples also have a low TiO_2 content but crystallize normal perovskite as a late phase. The bulk compositions of Samples 1370 and 1760 have a high CaO/MgO ratio and a low SiO_2 content (Table VII) compared with the other (representative) samples. However, these differences are probably more important in controlling the crystallization of merwinite instead of forsterite, than in controlling the pseudo-perovskite.

This suggests that the residual liquid compositions of the slags, and their products of crystallization, should be considered in terms of the system $CaO-MgO-Al_2O_3-TiO_2-SiO_2$. Unfortunately, the phase diagram has not been determined for this sytem.

8.2. Fractional crystallization

The high-temperature experiments have discounted (a) solid solution, (b) liquid immiscibility, and (c) eutectic growth as possible explanations of the pseudo-perovskite phase. However, the crystallization of blast-furnace slags is a non-equilibrium process, as judged by (i) the compositional zoning in melilite, and (ii) the appearance of up to six phases in this essentially five-component ($CaO-MgO-Al_2O_3-TiO_2-SiO_2$) system. Nurse and Midgley [4] studied a wide range of blast-furnace slags, and showed that the residual liquids crystallize independently of the bulk composition so leading to the formation of new phases such as diopside, wollastonite, and anorthite. This suggests that pseudo-perovskite could be accounted for as a product of fractional crystallization, although such an origin does not

TABLE VIB Calculated composition of the silicate component in the pseudo-perovskite of Table VIA

	Composition in oxides	Number of cations for 3 oxygens		
SiO_2	27.30	Si	0.56	0.98
Al_2O_3	17.30	Al	0.42	
MgO	9.05	Mg	0.27	1.25
MnO	5.09	Mn	0.08	
CaO	41.26	Ca	0.90	
Total	100.00			

TABLE VII Bulk chemical compositions of some ferrous blast-furnace slags

	Composition in oxides						
	1370	1760	1369	1393	1385	1388	1748
SiO_2	29.99	31.84	33.74	32.99	33.70	34.28	30.82
Al_2O_3	12.11	12.56	10.64	10.19	11.26	11.84	13.46
TiO_2	0.77	0.31	1.42	2.16	0.83	0.92	0.30
MgO	11.70	9.11	11.80	12.62	10.75	10.47	9.39
CaO	41.66	43.14	36.09	34.91	38.98	37.68	41.86
K_2O	0.34	0.58	0.94	1.21	0.68	0.92	0.57
MnO	0.23	0.20	1.65	3.17	0.88	0.83	0.27
P_2O_5	0.10	0.09	0.26	0.56	0.11	0.12	0.09
Na_2O	0.56	0.22	1.06	1.41	0.92	1.68	0.21
FeO	0.02	0.02	0.02	0.02	0.02	0.02	0.02
$Fe_{metallic}$	0.04	0.10	0.37	0.13	0.06	0.06	0.27
S	4.68	3.30	4.01	1.99	3.02	2.90	3.50
Sum	102.20	101.47	102.01	101.36	101.21	101.72	101.76
O=S	2.34	1.65	2.00	0.99	1.51	1.45	1.75
Total	99.86	99.82	100.01	100.37	99.70	100.27	99.01

Merwinite crystallizes in samples 1370, 1760, 1393, 1385 and 1748. Forsterite crystallizes in samples 1369 and 1388. There is no TiO_2-rich phase in sample 1748.

explain the causes for the intergrowth of perovskite and wollastonite.

8.3. Origin of wollastonite

In the system $CaO–MgO–Al_2O_3–SiO_2$ there is a thermal divide which prevents the compositions of blast-furnace slags evolving towards wollastonite: this would prevent the pseudo-perovskite being a product of fractional crystallization. However, there is a possibility that TiO_2 may have the relatively drastic effect of altering compatibility relations, so that wollastonite can crystallize from these slags. Thus, pseudo-perovskite is produced by fractional crystallization in the five-component system.

8.4. Concluding remarks

There is no conclusive experimental evidence to prove that the pseudo-perovskite is produced by fractional crystallization, although it appears the most likely explanation. The absence of pseudo-perovskite in other samples would then be explained by the failure of residual liquids to enter the field of wollastonite crystallization. This proposed origin does not explain the rounded shape, chemistry, and texture. Experimental work at atmospheric pressure on the system $CaO–MgO–Al_2O_3–TiO_2–SiO_2$ would be a valuable contribution to the understanding of pseudo-perovskite. However, some proposals can be made as to the textural features and the chemistry of the pseudo-perovskite.

8.4.1. The rounded shape

The shapes of minor mineral phases at grain boundaries depend on the interfacial energies, interfacial strains, and the requirements for space-filling. The roundness may represent an attempt by the pseudo-perovskite (the minor phase) to form a low-energy shape along the grain boundaries of melilite, merwinite, and monticellite.

8.4.2. Texture

The texture remains unresolved, although the fibres of wollastonite may represent the most energetically efficient form for crystallization on this scale. There is little understanding of the conditions controlling the formation of fibres.

8.4.3. Chemistry

If all the calculated silicate component (Table II) is a wollastonite, it would represent approximately wollastonite$_{50}$diopside$_{50}$ solid solution ($Wo_{50}Di_{50}$). Shinno [5] showed that wollastonite of the series between Wo_{100} and $Wo_{85}Di_{15}$ can be synthesized stably, but that if it is richer in the diopside component then it becomes metastable.

Acknowledgements

The author is grateful to the British Steel Corporation (Port Talbot Works) for permission to publish this paper. The technical assistance of Dr N. Charnley, Messrs C. R. Fagg, P. J. Jackson, K. A. Parrish, M. Slater, and the late R. A.

Holland is particularly acknowledged. The author is indebted to Drs B. C. M. Butler and D. G. Fraser for help with the high-temperature furnace experiments. This work was supported by the NERC and supervised by Dr B. C. M. Butler.

References

1. E. F. OSBORN, R. C. DEVRIES, K. H. GEE and H. M. KRANER, *J. Met.* **6**, (1954) 3.
2. A. E. RINGWOOD and A. MAJOR, *Earth Planet. Sci. Lett.* **12** (1971) 411.
3. R. C. DEVRIES, R. ROY and E. F. OSBORN, *J. Amer. Ceram. Soc.* **38** (1955) 158.
4. W. H. NURSE and H. G. MIDGLEY, *Silicates Ind.* **16** (1951) 211.
5. I. SHINNO, *Min. J. Jpn.* **7** (1974) 456.

Received 25 May
and accepted 14 September 1982